Synthesis and Solution Conformation of Cyclo[RGDRGD]: A Cyclic Peptide with Selectivity for the αVβ3 Receptor

Kevin Burgess* and Dongyeol Lim

Department of Chemistry, Texas A & M University, College Station, Texas 77843-3255

Shaker A. Mousa

DuPont Merck, Experimental Station, P.O. Box 80400, Wilmington, Delaware 19880-0400

Received April 9, 1996[⊗]

Three peptides, cyclo[RGDRGD], cyclo[RGDRGd] (d = D-Asp), and the linear sequence RGDRGD, were prepared via solid phase syntheses. These were tested in binding assays based upon the αIIb/β3-fibrinogen and the αVβ3-vitronectin interactions and found to be selective for the αVβ3 integrin. The αVβ3-vitronectin is important in bone regeneration, hence the compounds were also tested in an osteoclast regeneration assay; all three compounds, cyclo-[RGDRGD], cyclo[RGDRGd], and RGDRGD, showed modest activities. Molecular modeling, NMR, and CD studies were undertaken to elucidate the conformational preferences of cyclo-[RGDRGD] in aqueous solutions. Results from these studies strongly suggest that the molecule tends to adopt a type I β-turn conformation with a relatively short distance between the Asp and Arg side chains. These observations are in harmony with the first correlations made between αVβ3 selectivity and solution conformation for a peptide ligand (Pfaff, M.; *et al. J. Biol. Chem.* **1994**, *269*, 20233).

Some peptides and proteins, including fibrinogen and vitronectin, modulate cellular recognition phenomena by perturbing cell−cell and cell−matrix interactions. Critical to these processes are interactions of the -Arg-Gly-Asp- (RGD) sequence on the protein with cell surface integrins.[1] The initial focus of investigations in this area provided materials which block interactions of fibrinogen with the platelet αIIb/β3 receptor, and some compounds emerging from these studies are now in clinical trials for suppression of platelet aggregation. Subsequently, the emphasis of fundamental research in this area has shifted to other RGD receptors. One of these is αVβ3, the receptor for vitronectin. Osteoclasts, cells responsible for the bone resorption step in the skeletal repair process, express a relatively high density of αVβ3 integrins, hence it is possible that blocking this particular receptor could be exploited for the treatment of osteoporosis.[2] Other studies indicate that the αVβ3 integrin is crucial to angiogenesis,[3] a key step in solid tumor growth,[4,5] and it also has a central role in some diseases which lead to blindness and to inflammation.[6] This paper describes a synthesis of a relatively simple RGD derivative which has selectivity for the vitronectin receptor, and its preferred conformation in an aqueous environment.

Synthesis of the Peptides

At the onset, we were looking for a novel but relatively simple cyclic peptide containing the RGD sequence, and were surprised to find that cyclo[RGDRGD] had not been reported. Retrosynthetic analyses for this sequence shows there are three possible amide bonds that could be selected for the final ring closure step. These three possible disconnections are likely to give different yields for this cyclization process,[7] but it was impossible to predict with certainty which would be optimal. Consequently, the approach we initally used involved attachment of FMOC-Asp-ODmb (Dmb, 2,4-dimethoxybenzyl)[8] to Wang resin via the amino acid side chain. This permitted cyclization on the solid phase after elongation of the peptide using standard coupling procedures (BOP, HOBt).[9] Two major products were formed via this procedure, in a ratio of 1.7:1. In an alternative approach, FMOC-Asp(O^{t}Bu) was attached to 4-methylbenzhydrylamine (MBHA) resin via the highly acid labile 4-(hydroxymethyl)-3-(methoxyphenoxy)butyrate (HMPB) linker;[10] cleavage from the resin, cyclization in solution, and then deprotection gave the same two products, in a ratio of 4.3:1. Separation of these peptides was achieved by preparative, reverse phase HPLC.

Mass spectroscopic analyses proved that the two products formed in the syntheses described above were isomeric, and both had the molecular mass anticipated for the desired product cyclo[RGDRGD]. Cyclo-[RGDRGD] is C_2 symmetric; it has a relatively simple one-dimensional proton NMR spectrum and emerged as the predominant compound arising from both synthetic routes. The minor product plainly is not C_2 symmetric. Spectroscopic data for this material is consistent with the structure cyclo[RGDRGd] (d = D-Asp). It seems probable that this would arise via racemization of the supported Asp ester during the peptide couplings, although racemization at an Arg residue cannot be excluded on the basis of the data currently available. Structures derived from succinimide intermediate formation at an Asp residue[11,12] fit the spectral data less well than cyclo[RGDRGd]. Subsequently, we have found that samples in the cyclo[RGDRGD] series could be formed without contamination with any one significant byproduct via solid phase syntheses beginning with coupling of Gly to HMPB-MBHA resin, cyclization in solution, then side chain deprotection. This supports the suggestion that epimerization of Asp is facile in both routes used originally.

[⊗] Abstract published in *Advance ACS Abstracts,* October 1, 1996.

S0022-2623(96)00276-2 CCC: $12.00

Table 1. Inhibition Activities of the RGDRGD Derivatives

	IC_{50} (μM)	
	$\alpha V\beta 3$-vitronectin	$\alpha IIb/\beta 3$-fibrinogen[a]
cyclo[RGDRGD]	0.14 ± 0.02	>100
cyclo[RGDRGd]	0.32 ± 0.03	>100
RGDRGD	0.07 ± 0.01	>100
cyclo[RGDfV]	0.01 ± 0.01	>100
DMP728	>10	0.020 ± 0.001

[a] Percentage inhibition of human platelet aggregation ($\alpha IIb/\beta 3$-mediated) for cyclo[RGDRGD], cyclo[RGDRGd], and RGDRGD were 6%, 13%, and 7%, respectively. DMP728 is the cyclic compound (D-2-aminobutyryl-*N*-methyl-L-arginylglycyl-L-aspartyl)-3-aminomethylbenzoic acid.[23,24] This compound simultaneously run as a control in this same assay gave a 50% inhibition at 20 nM concentration.

In retrospect, the epimerization difficulties described above had the unforeseen advantage of affording cyclo-[RGDRGd] for testing. The linear hexapeptide RGDRGD was also prepared to give a second set of pharmacological data to compare with that derived from cyclo-[RGDRGD].

Receptor Binding and Osteoclast Generation Assays

Table 1 gives inhibition activities for cyclo[RGDRGD], cyclo[RGDRGd], and RGDRGD. All three peptides gave significant inhibition of the $\alpha V\beta 3$-vitronectin interaction such that their IC_{50} values were in the 70−320 nM region and extremely good selectivity for this receptor in comparison with the $\alpha IIb/\beta 3$-fibrinogen interaction. In the same Elisa assay, a peptide which is known to be selective for the vitronectin receptor, cycloRGDfV,[13,14] had an IC_{50} of 0.050 μM.[15] On a cellular level, cyclo-[RGDRGD], cyclo[RGDRGd], and RGDRGD gave insignificant inhibition of platelet aggregation.

Cyclo[RGDRGD], cyclo[RGDRGd], and RGDRGD were also tested in an osteoclast regeneration assay, wherein echistatin has an IC_{50} of 5−10 μM.[16] Each dose was tested in quadruplicate. The IC_{50}'s of cyclo[RGDRGD], cyclo[RGDRGd], and RGDRGD were 48 ± 9, 34 ± 6, 57 ± 9 μM.

Conformation of Cyclo[RGDRGD] in Aqueous Solution

A combination of molecular simulations, NMR, and CD studies in aqueous media was used to elucidate conformational preferences for cyclo[RGDRGD]. The quenched molecular dynamics (QMD)[17,18] protocol was used to simulate the conformations of these molecules. The key features of these experiments were as follows. After an initial molecular mechanics minimization of the (almost arbitrary) conformation initially inputted, a temperature of 1000 K was simulated for 1000 ps. Coordinates were downloaded every 1 ps throughout this dynamics run to generate 1000 "high energy conformers". These were separately subjected to molecular mechanics minimization (a constant dielectric of 80 was used throughout), giving 1000 "low-energy conformers". Twenty-nine structures within 6 kcal/mol of the lowest energy conformer observed (30 overall) were analyzed further as a basis for predicting the preferred solution conformations.

Figure 1 consists of two sets of overlaid line diagrams for the 30 preferred conformations that were generated in the QMD simulation. In Figure 1a the backbone atoms constituting the main chain of the cyclic peptide

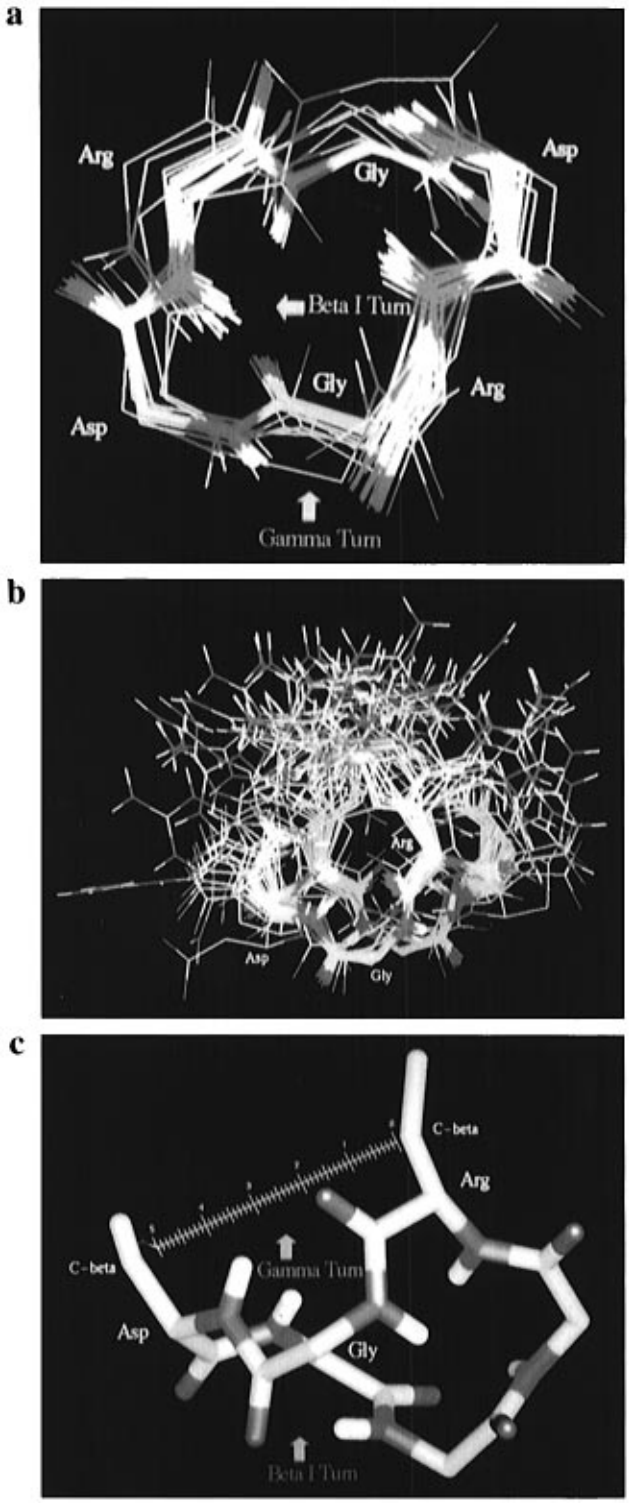

Figure 1. Overlaid minimum energy conformations of cyclo-[RGDRGD], generated by QMD, in (a) plan view and (b) side view. (c) Averaged favored conformer.

are shown in a plan view. All the conformers superimpose to within a relatively small deviation; hence the simulation suggests a single family of conformations is favored. This is also evident from ϕ,ψ dot plots for all three residue types (see the Supporting Information) wherein these critical bond vectors are clustered in relatively small areas of conformational space (approximate centers of ϕ,ψ distribution are as follows: Arg, +20°, −110°; Gly, +80°, −70°; Asp, −65°, −30°). The overlay shown in Figure 1a shows the main chains tend to adopt a distorted elliptical orientation. A side

Table 2. Comparison of Bond Vectors from NMR with Those Simulated in the QMD Study, and Selected Typical Dihedrals

contact[a]	ROE intensity	simulated distance (Å)	$^3J_{N\alpha}$ (Hz)	calculated ϕ (deg)[b]	simulated ϕ,ψ (deg)[c]	typical dihedrals (deg)[25] type-I β	γ
$R_{N\alpha}$	W	2.89	8.0	−91	−104, 24	−90, 0	
R_N–G_N	VW	2.46					
G_N–αRe	M	2.37	5.5	89	90, −69	–	80, −65
G_N–αSi	W	2.93	5.5	89	90, −69	–	80, −65
G_N–D_N	VW	3.50					
G_α–D_N	M	2.28					
G_α–D_N	W	3.40					
$D_{N\alpha}$	W	2.83	7.0	−82	−71, −23	−60, −30	
D_N–R_N	W	2.51					
D_α–R_N	W	3.31					
D_β–R_N	VW	3.86					

[a] The following examples illustrate the nomenclature used: $R_{N\alpha}$, ArgN*H*-C$_\alpha$*H*; R_N–G_N, ArgN*H*-GlyN*H*; G_α–D_N, GlyC$_\alpha$*H*–AspN*H*; D_β–R_N, AspC$_\beta$*H*–ArgN*H*. [b] Calculated on the basis of the Karplus equation;[26,27] in each case there are two or more alternatives, but only the most relevant calculated value is shown. [c] Measured from the averaged favored conformer in the QMD experiments.

view of the overlaid structures, which includes the side chains, is shown in Figure 1b. Together these two perspectives show that the main chain tends to adopt a dish-shaped conformation with a C_2 axis of symmetry perpendicular to the center of the dish. A pair of hydrogen bonds span the ring; these are formed via projection of the proximal Gly-N*H* to the distal Gly-C*O* and vice versa. The averaged coordinates for the favored conformers (henceforth referred to as "the averaged favored conformer") gives a Gly-N*H* to distal Gly-C*O* contact of 2.53 Å. These hydrogen bonds form a pair of rings which encapsulate the Arg and Asp residues on either side of the dish in type-I β-turns. There is also a second pair of hydrogen bonds linking the Asp-N*H* and the nonadjacent Arg-C*O* (the H···O distance in the consensus structure is 2.24 Å). The amide bonds which provide these acceptor and donor atoms are oriented in such a way that the H-bonds lie on the exterior of the dish. Two γ-turns, each centered about a Gly residue, arise from these hydrogen bonds. Side chains for the Asp and Arg residues are arrayed above the dish. There are perceptible preferences with regard to the orientation of the C$_\alpha$–C$_\beta$ bonds, but the conformational overlay becomes increasingly frayed with respect to bonds further down the side chains.

Two-dimensional NMR experiments were performed to probe the relevance of the simulated preferred conformations to the conformation preferences of cyclo-[RGDRGD] in an aqueous environment. Throughout, 50 mM phosphate buffer from 9:1 H_2O/D_2O was used for these NMR studies. Table 2 compares relative volume integrals for cross peaks observed in the ROESY spectrum of compound **1** with distances measured from the structure generated by averaging the coordinates for the 30 most favored conformers generated in the QMD experiment (distances derived from the lowest energy conformer detected are similar). For two N*H* to N*H* contacts (R_N–G_N and D_N–R_N, Table 2) the ROE intensities are weaker than would be expected based on the simulated conformation. Diminished cross peak intensities could arise from partial N*H* to N*D* exchange on the time scale of the experiment, broad line widths of the NH peaks, and/or unfavorable correlation times. Consequently, the discrepancies between the volume integrals and the predicted contact data could be due to unfavorable features of the ROESY experiment rather than genuine violations. There were no discrepancies of the more serious kind, i.e., wherein a strong ROE cross peak is associated with a contact that is predicted to be weak. In summary, the ROE data is consistent with the family of preferred conformations from the QMD experiments.

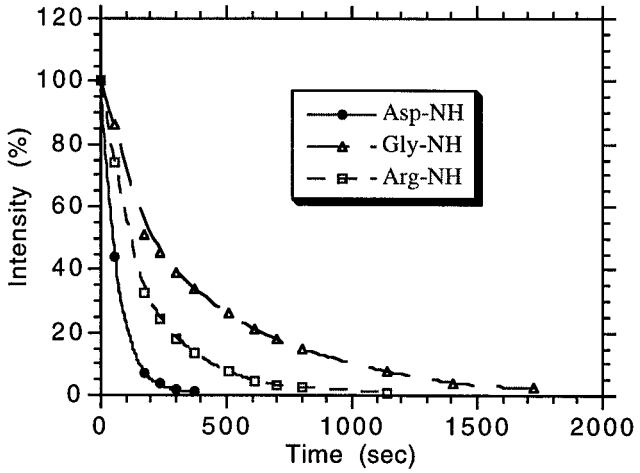

Figure 2. H/D exchange profiles for the amide protons of cyclo[RGDRGD] measured at 25 °C in D_2O.

Table 2 compares bond angles from the simulated averaged favored conformer, with ϕ angles calculated from coupling constants. Typical dihedrals for a type-I β-turn and for a γ-turn are shown for comparison. Throughout, one of the calculated ϕ values and those in the averaged favored conformer have a reasonable correspondence (largest discrepancy is 13°).

Figure 2 shows H/D exchange profiles for the three types of amide protons in cyclo[RGDRGD]. The relative rates of exchange follows the order Asp-N*H* > Arg-N*H* > Gly-N*H* and is consistent with the preferred conformations shown in Figure 1 for the following reasons. Slow exchange of the Gly-N*H* could be indicative of the hydrogen-bonding relationship which this proton forms (to give the β-turns) and of the orientation of this proton toward the center of the dish shape formed by the peptide main chain. The Arg-N*H* proton, i.e., that with the intermediate H/D exchange rate, is also predicted to be within the dish structure, but is not involved in a H-bonding interaction. Relatively fast exchange could be a consequence of projection of this proton out into the aqueous medium causing it to exchange rapidly despite the stabilizing effect of the Asp-N*H* to Arg-C*O* hydrogen bond.

Near-UV CD spectra of the RGD derivatives are shown in Figure 3. Predictably, the CD spectrum of the linear peptide RGDRGD shows the least indication of adopting any detectable secondary structure in solu-

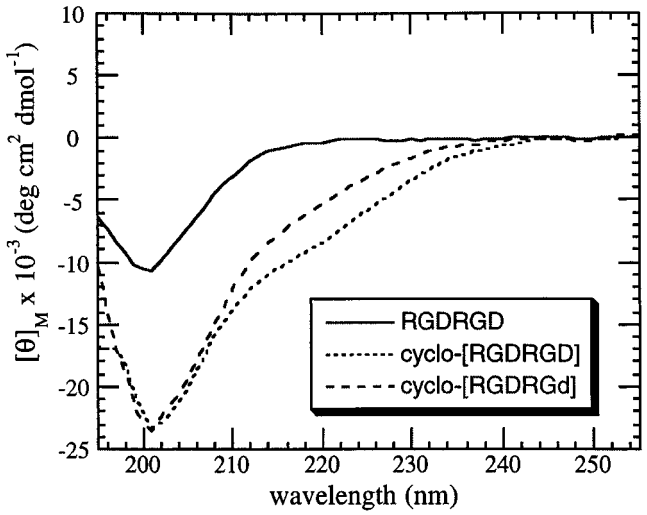

Figure 3. Near-UV CD spectra for the RGDRGD derivatives.

tion: it shows a relatively small negative elipticity at 200 nm. The two cyclic peptides, however, show more evidence of ordered solution conformations. Their spectra show a large negative elipticity at approximately 201 nm, and a shoulder at around 218 nm which is more prominent for cyclo[RGDRGD]. These two negative maxima are characteristic of a type-I β-turn in a short peptide. The spectra shown in Figure 3 are very similar to those reported for another peptide system which is thought to contain a type-I β-turn motif.[19]

Discussion

At the present time, reports of compounds that bind selectively to the $\alpha V\beta 3$ integrin are rare.[15,20−22] Until recently, the best documented example was cyclo-[RGDfV], a cyclic pentapeptide that binds to $\alpha V\beta 3$ with an IC_{50} of 0.049 μM.[13] The conformation of cyclo-[RGDfV] in aqueous DMSO has been studied in detail.[13,14] There is a striking similarity between the favored conformations of cyclo[RGDRGD] and cyclo-[RGDfV] insofar as both molecules have a γ-turn motif centered around the Gly residue. It has been suggested that the binding site of $\alpha V\beta 3$ is narrower or more restricted than that of $\alpha IIb/\beta 3$; hence ligands that bind the former selectively are more constrained and, specifically, tend to have no more than 0.67 nm between the C_β atoms of the Asp and Arg residues.[13] These predictions agree well with the results described here. Remarkably, the separation between the Asp and Arg C_β atoms in the averaged favored conformer is 0.58 nm. In both peptides it may be that the γ-turn has a pivotal role; these studies indicate that it pinches the RGD array, bringing the Asp and Arg side chains closer together (Figure 1c). Neither cyclo[RGDRGD] nor RGDRGD have hydrophobic residues flanking the RGD sequence hence these are not critical for binding to $\alpha V\beta 3$. The fact that the linear peptide RGDRGD is the most active in this series with respect to binding to the $\alpha V\beta 3$ receptor implies that the conformations adopted by cyclo[RGDRGD], though suitable, are not optimal, and that linear RGDRGD may be able to fold into a conformation that fits the receptor even more closely. There is also an alternative explanation for the activity of linear RGDRGD which is based on the hypothesis that the backbone conformation is not as important as the orientation of the guanidine and acid side chains. Specifically, in the linear peptide the free carboxylic acid on the *C*-terminus may be substituting for the Asp side chain pharmacophore, and the fact that this is closer to the guanidine than the Asp side chain may lead to increased activity.

The osteoclast inhibition data for all three hexapeptides prepared and tested in this work indicates that the compounds have some activity in this assay, but they are not as potent as the naturally occurring peptide echistatin.

After the work presented in this paper was originally submitted, three other peptides with good affinity (IC_{50} = 0.020, 0.036, 0.013 μM, in Elisa the same assay that is described in this paper) and high selectivity for the $\alpha V\beta 3$ receptor were reported, specifically cyclo(*X*-Arg-Gly-Asp-Mamb) where *X* = Ala, Aib, and Pro, respectively {Mamb = *m*-(aminomethyl)benzoic acid}.[15,20−22] The most active of these has a preferred type-I β-turn conformation which forms a scaffold upon which projects the Arg and Asp side chains into a relatively close proximity.

The observations of Bach and co-workers working with cyclo(*X*-Arg-Gly-Asp-Mamb) peptides as described above,[15] those of Kessler *et al*. with regard to cyclo-[RGDfV],[13] and the data described in this paper strongly support three assertions. These are as follows: (i) the $\alpha V\beta 3$ receptor recognizes conformations wherein the Arg and Asp side chains are much closer than in the bioactive conformation for binding to the $\alpha IIb/\beta 3$ receptor; (ii) a type-I β-turn is a good template for presenting these side chains in the desired orientation; and (iii) hydrophobic residues flanking the RGD sequence are not a prerequisite for binding to the $\alpha V\beta 3$ receptor, although they may impart effects which enhance this interaction.

Experimental Section

Syntheses of Cyclo[RGDRGD] and Cyclo[RGDRGd]. First Method. The cyclic peptides were prepared by stepwise couplings of FMOC-amino acid derivatives on Wang resin. The (4-methoxy-2,3,6-trimethylphenyl)sulfonyl (Mtr) group was used as side chain protection for arginine (i.e., FMOC-Arg-(Mtr) was used). The *tert*-butyl (^{t}Bu) group was used for side chain protection of aspartic acid, and the main chain carbonyl was protected using the 2,4-dimethoxybenzyl (Dmb) group. Manual peptide synthesis was carried out in a 30 mL vessel fitted with a coarse glass frit using a wrist action shaker (Burrel, Model 75). The reagents were added manually. All reactions were carried at 25 °C unless otherwise specified. FMOC deprotection was performed by shaking the resin twice with 20% piperidine in DMF (5 mL, 3 min and 5 mL, 7 min); DMF washing cycles (10 × 1 min, *ca*. 10 mL) were performed after each coupling and deprotection.

The symmetric anhydride of FMOC-Asp-ODmb (commercially available from BACHEM Bioscience Inc.) was prepared by mixing 0.441 g of the amino acid (0.9 mmol) and diisopropylcarbodiimide (DIPCDI) (72 μL, 0.45 mmol) in CH_2Cl_2 (5 mL). The mixture was stirred for 1 h and then used for the coupling reaction without further purification. Wang resin (0.600 g of 0.5 mmol g^{-1} capacity) was first swelled in DMF (*ca*. 10 mL) for 2 h and then reacted with (FMOC-Asp-ODmb)$_2$O (0.45 mmol, 1.5 equiv) and DMAP (36.7 mg, 0.30 mmol) in DMF (5 mL). The mixture was then shaken for 1 h and washed. The resin was capped using acetic anhydride (0.43 mL) and DMAP (36.7 mg) in DMF (2 mL) for 1 h. The FMOC protecting group was removed, and the resin was washed as previously. Five cycles of deprotection and coupling {FMOC-amino acids (3 equiv, 0.9 mmol), BOP (398 mg, 0.9 mmol, 3 equiv), HOBt (122 mg, 3 equiv, 0.9 mmol)} were then performed, followed by Dmb ester group removal using 1%

TFA solution in CH_2Cl_2 (6 × 5 min, 15 mL). After removal of the final FMOC protecting group, the resin was washed thoroughly with DMF and HOBt/DMF to remove any trace of piperidine. A sample of 202 mg of the resin bound peptide was saved to make a linear RGDRGD. Cyclization of the resin bound linear peptide (603 mg) was done with BOP (177 mg, 0.4 mmol), HOBt (54 mg, 0.4 mmol), and DIPEA (52 μL, 0.3 mmol).

Cleavage of the peptide from the resin was affected using the following procedure. The resin was completely dried under high vacuum, and then a mixture of phenol (1.0 mL), 1,2-ethanedithiol (0.5 mL), thioanisole (1.0 mL), deionized water (1.0 mL), and trifluoroacetic acid (16.5 mL) was precooled to 0 °C and added to the resin in a shaker. The reaction mixture was agitated at 25 °C for 21 h. The resin was then filtered and washed with trifluoroacetic acid (25 mL) and then with CH_2Cl_2 (15 mL). The filtrate was evaporated to *ca.* 2 mL. Et_2O (30 mL) was added, and the resulting precipitate was filtered and then washed with Et_2O (5 × 10 mL). The crude peptide was further purified by preparative RP-HPLC (Vydac C18 column, 22 mm × 25 cm, 10 μm) with a linear gradient obtained by mixing solvent A (0.1% TFA in water) and solvent B (0.1% TFA in acetonitrile). The gradient was programmed to increase from 3 to 5% B over 35 min with a flow rate of 6 mL min^{-1}. The peaks with retention times of 25.6 min (major) and 31.3 min (minor) were collected and lyophilized. The ratio of two peaks in the HPLC trace was 1.7 to 1.0. The major peptide (TFA salt) was obtained as a very hygroscopic powder (9.5 mg, 5.4% based on the resin used) and proved to be cyclo-[RGDRGD] by NMR and MS. +FAB/DP (thioglycerol), *m/e* calcd for $C_{24}H_{40}N_{12}O_{10}$ 656, found 657 for $[M + H]^+$. The minor peptide was obtained (3.5 mg, 2%) and showed the same mass spectrum. NMR assignments for both compounds are listed in Table S1 of the Supporting Information.

Second Method. The symmetric anhydride of FMOC-Asp-(^{t}Bu)-OH was prepared by mixing 0.704 g of the amino acid derivative (1.71 mmol) and diisopropylcarbodiimide (DIPCDI) (134 μL, 0.855 mmol) in CH_2Cl_2 (10 mL). The mixture was stirred for 1 h and used for coupling without purification. HMPB-MBHA resin (1.0 g of 0.57 mmol g^{-1} capacity, Nova-Biochem) was swelled in DMF (*ca.* 10 mL) for 1 h. Coupling of FMOC-Asp(^{t}Bu)-OH was performed by mixing (FMOC-Asp-(^{t}Bu)-)$_2$O (0.855 mmol, 1.5 equiv) with the preswelled HMPB-MBHA resin, DMAP (7 mg, 0.057 mmol), and DIPCDI (108 mg, 0.855 mmol) in DMF (5 mL), and then the mixture was stirred for 12 h at 0 °C and washed. The resin was end-capped using acetic anhydride (0.817 mL) and DMAP (69.7 mg) in DMF (5 mL) for 30 min. Five cycles of deprotection and coupling were done as described in the first method. FMOC-protected peptide was cleaved from the resin using a 1% TFA solution in CH_2Cl_2 (8 × 5 min, 10 mL), and the cleavage was checked by TLC. The combined solution was concentrated and then added dropwise to the water (60 mL) with stirring. The resulting solid was filtered and dried to give 770 mg of crude peptide. Removal of FMOC was carried with 10% diethylamine solution in CH_3CN (27.5 mL). After 2 h of stirring, the reaction solution was concentrated, CH_3CN (20 mL) was added, and the mixture was evaporated twice to remove traces of diethylamine and then triturated with Et_2O to remove dibenzofulvene. After being filtered and washed with Et_2O, 568 mg of white solid was obtained, A sample of 100 mg of the this material was saved to make a linear RGDRGD. Cyclization of the peptide (468 mg) was done with BOP (1064 mg, 6.2 equiv), HOBt (326 mg, 6.2 equiv), and DIPEA (210 μL, 3.1 equiv). After 36 h of stirring, crude product was extracted with EtOAc, and the organic layer was washed with water and brine, dried over $MgSO_4$, and concentrated to give 375 mg of crude cyclized product as a white solid. Deprotection and purification of the peptide were performed as explained in the first method. The ratio of two peaks in HPLC trace was 4.3 to 1.0. A scheme outlining the syntheses of the peptides is provided in the Supporting Information.

The linear peptide RGDRGD was obtained by the deprotection of the intermediate before cyclization in the method described above; *m/e* calcd for $C_{24}H_{42}N_{12}O_{11}$ 674, found 675 for $[M + H]^+$.

Platelet Aggregation Assays by Light Transmittance Aggregometry. In a purified αIIb/β3 assay as described by Mousa *et al.*,[23] preliminary experiments showed DMP728 had an IC_{50} of 0.1 nM while all the other compounds tested had IC_{50}'s of >10 μM. The following, more convenient, clotting assay was therefore used since the activities of the target compounds were so low. This assay was repeated four times to obtain the data shown in Table 1. Venous blood was obtained from healthy human donors who were drug- and aspirin-free for at least 2 weeks prior to blood collection. The blood was collected into citrated Vacutainer tubes and centrifuged for 15 min at 150*g* (850 RPM in a Sorvail RT6000 Tabletop Centrifuge with H-1000 B rotor) and at room temperature, and then the platelet-rich plasma (PRP) was removed. The remaining blood was centrifuged for 15 min at 1500*g* at room temperature, and the platelet-poor plasma (PPP) was removed. Samples were assayed on a PAP-4 platelet aggregation profiler, using PPP as the blank (100% transmittance). An aliquot of 200 μL of PRP (5 × 108 platelets/mL) were added to each micro test tube, and transmittance was set to 0%. Aliquots of 20 μL of the platelet agonists including ADP (100 μM) were added to each tube, and the aggregation profiles were plotted (percent transmittance versus time). The test agent (20 μL) was added at different concentrations prior to the addition of the different platelet agonists. The results were expressed as percent inhibition of agonist-induced platelet aggregation.

Purified αvβ3 Receptors Binding Assay. The following assay was repeated four times to obtain the data shown in Table 1. Purified receptor obtained from human placenta was diluted with coating buffer and coated (100 μL/well) in Costar (3590) high capacity binding plates overnight at 4 °C. The coating solution was discarded, and the plates were washed once with B buffer (50 mM Tris·HCl, 100 mM NaCl, 2 mM $CaCl_2$, 1 mM $MgCl_2$, 1 mM $MnCl_2$, pH 7.4) and then blocked with 200 μL/well of 1.0% BSA in B buffer for 30 min at room temperature. After the mixture was washed once with 1.0% BSA in B buffer, 100 μL of biotinylated vitronectin and 11 μL of either inhibitor or B buffer with 1.0% BSA were added to each well. After incubation for 30 min at room temperature, the plate was washed twice with B buffer and incubated for 1 h at 25 °C with anti-biotin alkaline phosphatase (100 μL/well) in B buffer containing 1.0% BSA. The plate was washed twice with B buffer, and then 100 μL of alkaline phosphatase substrate was added. The color developed at 25 °C, and the color development was terminated by adding 2 N NaOH (25 μL/well). Finally, the OD was read at 405 nm. For determination of IC_{50} values, the test compound was added at various concentrations prior to biotinylated vitronectin.

Osteoclast Generation Assays. The compounds were tested following the reported prodcedure.[16] Each concentration was tested in quadruplicate.

Molecular Modeling. The Quanta CHARMM (version 22) modeling package was used for the molecular simulations performed in this work. Extended atom representations of the nonpolar hydrogen atoms were used.

Quenched molecular dynamics simulations were performed using the standard parameters for the natural amino acids. Thus the molecule of interest, cyclo[RGDRGD] was built in an extended conformation with positive charges on the guanidine side chains and negative charges on the Asp side chains. These starting conformers were minimized using 200 steps of steepest descent (SD) and 1000 steps of the adopted basis Newton−Raphson method (ABNR) in a dielectric constant of 80 (representing water). The minimized structure was then subjected to dynamics simulations. Throughout, the equations of motion were integrated using the Verlet algorithm with a time step of 1 fs, and SHAKE was used to constrain all bond lengths containing polar hydrogens. Each individual peptide was heated to 1000 K over 10 ps by increasing the temperature by 10 K every 0.1 ps. The peptide was equilibrated for 10 ps at 1000 K, during which time a ±13 K temperature constraint was applied to the system. Molecular dynamics production runs were then performed in the micro-

canonical (NVE)ensemble for a total time of 1000 ps. The trajectories were saved every 1 ps, and a total of 1000 structures was produced. Each of the structures was thoroughly minimized using 200 steps of SD followed by ABNR until a RMS energy derivative of ≤ 0.0001 kcal mol^{-1} Å^{-1} was obtained. Extra H-bonding option was applied during the minimization.

Structures ≤ 6 kcal mol^{-1} of the global minimum were selected for further analyses. Previous studies, specifically of tuftsin (Thr-Lys-Pro-Arg) and Met-enkephalin (Tyr-Gly-Gly-Phe-Met), have shown that a 3−7 kcal mol^{-1} energy cutoff was sufficient to select the structures which gave reasonable agreement with the NMR data. In this work a 6 kcal mol^{-1} cutoff was selected, giving 30 structures for further analysis. The coordinates of the selected structures were reoriented by mass weighting an RMS calculation using peptide backbone atoms, averaged in Cartesian coordinates, and the protons were built on the heavy atoms using standard geometry. Finally, the interproton distances were calculated from these coordinates for comparisons of the simulated structures with the ROE data obtained in the NMR studies.

NMR Studies. NMR spectra were recorded on a Varian Unity+ 500 spectrometer (500 MHz). In the COSY/ROESY experiments, presaturation was carried out to suppress the water signal. The peptide (4.76 mM) was dissolved in a mixture of 10% D_2O and 90% H_2O containing potassium phosphate (50 mM, pH = 5.5). In the H−D exchange experiments, the peptide was dissolved in D_2O at 25 °C and the spectra was recorded at intervals after that.

One-dimensional (1D) ^{1}H-NMR spectra were recorded with a spectral width of 8000 Hz, 30 272 data points, 32 transients, and a 5 s acquisition time. Vicinal coupling constants were measured from the 1D spectra at ambient temperature. Temperature coefficients of amide protons were measured via several 1D experiments at 5−45 °C, adjusted in 10 °C increments with equilibration time of ≥10 min after successive temperature steps.

Two-dimensional (2D) spectra were taken at 25 °C with a spectral width of 8000 Hz. Through-bond connectivities were elucidated by DQF-COSY spectra, which were recorded with 512 t_1 increments and 32 scans per t_1 increments with 2 K data points at t_2.

Sequential assignments and proton−proton close contacts were elucidated by ROESY spectra, which were recorded with a 2 s relaxation delay, 512 t_1 increments, and 32 scans per t_1 increments with 2 K data points at t_2. The spin-lock field was generated by a continuous field. The carrier frequency was fixed to water signal, and resonance offset compensation was applied. ROESY experiments with mixing times of 75, 100, 200, 300, and 500 ms were recorded to identify peaks caused by spin diffusion. Both DQF-COSY and ROESY data were zero-filled to 2K × 2K data sets and Gaussian transformed in both dimensions. The intensities of ROESY cross peaks were assigned as VS (very strong), S (strong), M (medium), W (weak), and VW (very weak) by the magnitude of volume integral. Cutoff distances from ROE data tend to be less than in the corresponding NOE experiments. Nevertheless, an upper level constraint of 5 Å is maintained in this study to ensure that the boundary conditions for comparisons of NMR and experimental data are not too severe.

CD Studies. The peptides were dissolved in 50 mM potassium phosphate buffer solution (pH 5.4). Concentrations were determined by comparing the HPLC integration at 214 nm detection with that of a RGDRGD sample of exactly determined concentration. The concentration range of the samples studies was 286−456 μM. The spectra shown were recorded on an Aviv model 62DS spectrometer.

Acknowledgment. We thank Drs. Gideon A. Rodan and Sevgi B. Rodan at Merck for organizing the osteoclast generation assays. We also thank Sharon Jackson (DuPont Merck) and Steve Silber (A & M) for helpful comments. The National Institutes of Health and The Robert A. Welch Foundation provided direct support for this research, and K.B. thanks the NIH for a Research Career Development Award and the Alfred P. Sloan Foundation for a fellowship. NMR facilities were provided by the NSF via the chemical instrumentation program.

Supporting Information Available: Scheme for the peptide syntheses, NMR chemical shift data, and ϕ,ψ scatter plots for the R, D, and G residues in the 30 lowest energy conformers from the QMD simulation of cyclo[RGDRGD] (3 pages). Ordering information is given on any current masthead page.

References

(1) Ruoslahti, E.; Pierschbacher, M. D. New perspectives in cell adhesion: RGD and integrins. *Science* **1987**, *238*, 491−7.
(2) Hruska, K. A.; Rolnick, F.; Huskey, M.; Alvarez, U.; Cheresh, D. Engagement of the osteoclast integrin alpha (v) beta (3) by osteopontin stimulates phosphatidylinositol 3-hydroxyl kinase activity. *Endocrinology* **1995**, *136*, 2984−92.
(3) Drake, C. J.; Cheresh, D. A.; Little, C. D. An antagonist of integrin alpha(v)beta(3) prevents maturation of blood vessels during embryonic neovascularization. *J. Cell Sci.* **1995**, *108*, 2655−61.
(4) Seftor, R. E. B.; Seftor, E. A.; Gehlsen, K. R.; Stetler-Stevenson, W. G.; Brown, P. D.; Ruoslahti, E.; Hendrix, M. J. C. Role of the alpha.v.beta.3 integrin in human melanoma cell invasion. *Proc. Natl. Acad. Sci. U.S.A.* **1992**, *89*, 1557−61.
(5) Brooks, P. C.; Stromblad, S.; Klemke, R.; Visscher, D.; Sarkar, F. H.; Cheresh, D. A. Antiintegrin alpha-v-beta-3 blocks human breast angiogenesis in human skin. *J. Clin. Invest.* **1995**, *96*, 1815−22.
(6) Friedlander, M.; Brooks, P. C.; Shaffer, R. W.; Kincaid, C. M.; Varner, J. A.; Cheresh, D. A. Definition of Two Angiogenic Pathways by Distinct α_v Integrins. *Science* **1995**, *270*, 1500−2.
(7) Cavelier-Frontin, F.; Pepe, G.; Verducci, J.; Siri, D.; Jacquier, R. Prediction of the Best Linear Precursor in the Synthesis of Cyclotetrapeptides by Molecular Mechanic Calculations. *J. Am. Chem. Soc.* **1992**, *114*, 8885−90.
(8) McMurray, J. S. Solid Phase Synthesis of a Cyclic Peptide Using Fmoc Chemistry. *Tetrahedron Lett.* **1991**, *32*, 7679−82.
(9) Felix, A. M.; Wang, C.-T.; Heimer, E. P.; Fournier, A. Applications of BOP Reagent in Solid Phase Synthesis II. Solid Phase Side-chain to Side-chain Cyclizations Using BOP Reagent. *Int. J. Pept. Protein Res.* **1988**, *31*, 231−38.
(10) McMurray, J. S.; Lewis, C. A. The Synthesis of Cyclic Peptides Using Fmoc Solid-Phase Chemistry and the Linkage Agent 4-(4-Hydroxymethyl-3-methoxyphenoxy)-butyric Acid. *Tetrahedron Lett.* **1993**, *34*, 8059−62.
(11) Bodanszky, M.; Natarajan, S. Side Reactions in Peptide Synthesis. II. Formation of Succinimide Derivatives from Aspartyl Residues. *J. Org. Chem.* **1975**, *40*, 2495−9.
(12) Liotta, L. J.; Gibbs, R. A.; Taylor, S. D.; Benkovic, P. A.; Benkovic, S. J. Antibody-Catalyzed Rearrangement of a Peptide Bond: Mechanistic and Kinetic Investigations. *J. Am. Chem. Soc.* **1995**, *117*, 4729−41.
(13) Pfaff, M.; Tangemann, K.; Müller, B.; Gurrath, M.; Müller, G.; Kessler, H.; Timpl, R.; Engel, J. Selective Recognition of Cyclic RGD Peptides of NMR Defined Conformation by αIIbβ3, αVβ3, and α5β1 Integrins. *J. Biol. Chem.* **1994**, *269*, 20233−8.
(14) Gurrath, M.; Müller, G.; Kessler, H.; Aumailley, M.; Timpl, R. Conformation/activity studies of rationally designed potent anti-adhesive RGD peptides. *Eur. J. Biochem.* **1992**, *210*, 911−21.
(15) Bach, A. C.; Espina, J. R.; Jackson, S. A.; Stouten, P. F. W.; Duke, J. L.; Mousa, S. A.; Degrado, W. F. Type II′ to Type I β-Turn Swap Changes Specificity for Integrins. *J. Am. Chem. Soc.* **1996**, *118*, 293−4.
(16) Wesolowski, G.; Duong, L. T.; Lakkakorpi, P. T.; Nagy, R. M.; Tezuka, K.; Tanaka, H.; Rodan, G. A.; Rodan, S. B. Isolation and Characterization of Highly Enriched Prefusion Mouse Osteoclastic Cells. *Exp. Cell Res.* **1995**, *219*, 679−86.
(17) Pettitt, B. M.; Matsunaga, T.; Al-Obeidi, F.; Gehrig, C.; Hruby, V. J.; Karplus, M. Dynamical Search for Bis-penicillamine Enkephalin Conformations. *Biophys. J.* **1991**, *60*, 1540−4.
(18) O'Connor, S. D.; Smith, P. E.; Al-Obeidi, F.; Pettitt, B. M. Quenched molecular dynamics simulation of tuftsin and proposed cyclic analogues. *J. Med. Chem.* **1992**, *35*, 2870−81.
(19) Bisang, C.; Weber, C.; Inglis, J.; Schiffer, C. A.; Gunsteren, W. F. v.; Jelesarov, I.; Bosshard, H. R.; Robinson, J. A. Stabilization

of Type-I β-Turn Conformations in Peptides Containing the NPNA-Repeat Motif of the *Plasmodium falciparum* Circumsporozoite Protein by Substituting Proline for (S)-α-Methylproline. *J. Am. Chem. Soc.* **1995**, *117*, 7904−15.

(20) Healy, J. M.; Murayama, O.; Maeda, T.; Yoshino, K.; Sekiguchi, K.; Kikuchi, M. Peptide Ligands for Integrin $\alpha_v\beta_3$ Selected from Random Phage Display Libraries. *Biochemistry* **1995**, *34*, 3948−55.

(21) Pasqualini, R.; Koivunen, E.; Ruoslahti, E. A peptide isolated from phage display libraries is a structural and functional mimic of an RGD-binding site on integrins. *J. Cell Biol.* **1995**, *130*, 1189−96.

(22) Koivunen, E.; Wang, B.; Ruoslahti, E. Phage libraries displaying cyclic peptides with different ring sizes: ligand specificities of the RGD-directed integrins. *Bio/Technology* **1995**, *13*, 265−70.

(23) Mousa, S. A.; Bozarth, J. M.; Forsythe, M. S.; Lorelli, W.; Thoolen, M. J.; Ramachandran, N.; Jackson, S.; Grado, W. D.; Reilly, T. M. Antiplatelet Efficacy and Specificity of DMP 728, a Novel Platelet GPIIb/IIIa Receptor Antagonist. *Cardiology* **1993**, *83*, 374−82.

(24) Mousa, S. A.; Bozarth, J. M.; Forsythe, M. S.; Jackson, S. M.; Leamy, A.; Diemer, M. M.; Kapil, R. P.; Knabb, R. M.; Mayo, M. C.; Pierce, S. K.; Grado, W. F. D.; Thoolen, M. J.; Reilly, T. M. Antiplatelet and Antithrombotic Efficacy of DMP 728, a Novel Platelet GPIIb/IIIa Receptor Antagonist. *Circulation* **1994**, *89*, 3−12.

(25) Creighton, T. E. In *Proteins: Structures and Molecular Properties*; W. H. Freeman and Company: New York, 1993.

(26) Pardi, A.; Wagner, G.; Wuthrich, K. Semi-empirical Karplus relations to determine ensemble-averaged dihedral angles. *Eur. J. Biochem.* **1983**, *137*, 445−54.

(27) Pardi, A.; Billeter, M.; Wüthrich, K. Calibration of the Angular Dependence of the Amide Proton-C^α Proton Coupling Constants, $^3J_{HN\alpha}$, in a Globular Protein. Use of $^3J_{HN\alpha}$ for Identification of Helical Secondary Structure. *J. Mol. Biol.* **1984**, *180*, 741−51.

JM960276A